Safe Optimization of Highway Traffic With Robust Model Predictive Control-Based Cooperative Adaptive Cruise Control

Carlos Massera Filho, *Student Member, IEEE*, Marco H. Terra, *Member, IEEE*, and Denis F. Wolf, *Member, IEEE*

***Abstract*— Road traffic crashes have been the leading cause of death among young people. Most of these accidents occur when the driver becomes distracted due to fatigue or external factors. Vehicle platooning systems, as cooperative adaptive cruise control, are one of the results of efforts devoted to the development of technologies for decreasing the number of road crashes and fatalities. Previous studies have suggested that such systems improve up to 273% highway traffic throughput and over 15% of fuel consumption if the clearance between vehicles in this class of roads can be reduced to 2 m. In this paper, we propose an approach that guarantees a minimum safety distance between vehicles taking into account the overall system delays and braking capacity of each vehicle. An $l\infty$-norm robust model predictive controller has been developed to guarantee the minimum safety distance is not violated due to uncertainties on the preceding vehicle behavior. A formulation for a lower bound clearance of vehicles inside a platoon is also proposed. Simulation results show the performance of the approach compared to a nominal controller when the system is subject to both modeled and unmodeled disturbances.**

***Index Terms*— Intelligent vehicles, advanced driver assistance systems, optimal control, robust control.**

I. Introduction

In RECENT years, both academia and industry have devoted efforts towards the development of assistance systems for improving the drivers comfort and/or decreasing the number of road accidents. Vehicle platooning systems, such as Adaptive Cruise Control (ACC) [2] and Cooperative Adaptive Cruise Control (CACC) [14], are examples of this class of systems through which a vehicle regulates its own velocity and distance to the vehicle ahead based on a sensor suite and wireless communication interfaces, respectively.

ACC systems have already reached consumer market through radar [2] and camera [12] technologies. Such interest in vehicle platooning has led to the development of vehicle-specific communication protocols, such as 802.11p [18] and DSRC [40] necessary for the development of CACC systems. Studies have shown that CACC can improve up to 273% road traffic throughput and significantly reduce fuel consumption [36] given a high market penetration [35], [37]. However, such improvements rely on the assumption CACC technology will significantly reduce the clearance between vehicles. In this proposed scenario, any disturbance in the preceding vehicle behavior might cause an accident. Therefore, stability, performance robustness and robustness against violating the minimum distance between vehicles must be ensured.

Model Predictive Control (MPC) is a class of optimization-based control algorithms which uses an explicit model of the controlled system to predict its future states [1]. MPC objective is to minimize a cost functional and maintain the system states and control inputs within a feasible set. The system dynamics are usually assumed to be known. Therefore, model mismatches or external disturbances are not considered. However, the disregard of such uncertainties may lead to poor closed-loop performance and the violation of state and control input constraints [32]. Robust Model Predictive Control (RMPC) addresses the poor closed-loop performance subject to uncertainties [3]. The main RMPC approach is based on Min-Max optimization, its objective is to obtain a control input sequence that minimizes a cost functional and to guarantee the feasibility of system states and control inputs when the system is subject to the worst-case disturbance.

In this paper we propose a cooperative adaptive cruise controller based on $l\infty$-norm robust model predictive controller which rejects uncertainties from the unknown preceding vehicle acceleration behavior and operates close to the minimum safety distance between vehicles. The main contributions of this work are the formulation of such CACC system and a novel formulation of the minimum safety distance between vehicles that incorporates the preceding vehicle braking capacity.

The remainder of the paper is organized as follows: Section II discusses related work; Section III presents the system modeling; Section IV describes the applications safety and comfort constraints; Section V addresses the formulation of the proposed controller; Section VI reports the experiments performed; finally, Section VII provides the final remarks.

II. Related Work

The recent development of systems based on vehicle-to-vehicle (V2V) communication has drawn growing interest from the research community due to improvements in communication bandwidth and processing power. Studies on

Manuscript received May 25, 2016; revised November 4, 2016 and February 8, 2017; accepted February 25, 2017. Date of publication May 19, 2017; date of current version October 30, 2017. This work was supported by FAPESP under Grant 2013/24542-7. The Associate Editor for this paper was J. Ploeg.

C. M. Filho and D. F. Wolf are with the Institute of Mathematics and Computer Science, University of São Paulo (e-mail: massera@icmc.usp.br; denis@icmc.usp.br).

M. H. Terra is with the São Carlos School of Engineering, University of São Paulo (e-mail: terra@sc.usp.br).

Color versions of one or more of the figures in this paper are available online at http://ieeexplore.ieee.org.

Digital Object Identifier 10.1109/TITS.2017.2679098

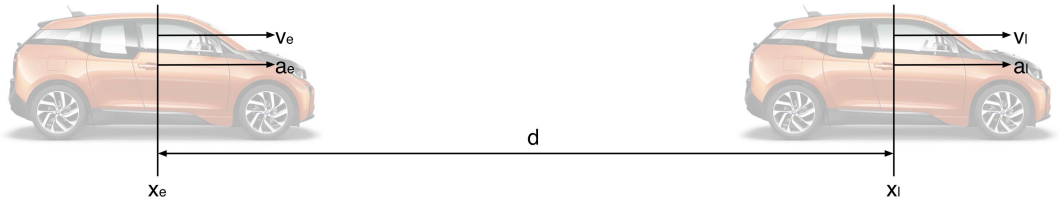

Fig. 1. Representation of the ego and preceding vehicle models.

communicating vehicles culminated in two editions of the Grand Cooperative Driving Challenge (GCDC) [4] held in 2011 and 2016, in which vehicles had to perform highway platooning tasks using embedded sensors and V2V communication [14].

The main goal of CACC systems is to track a leading vehicle with a given desired distance [10]. These systems can be classified by two properties: distance and information topology among vehicles. Constant vehicle distances (e.g. [27], [36]) and constant headway time (e.g. [26], [34]) are the two major vehicle distance policies. Whereas, predecessor following (PF), predecessor-leader following (PLF) and bidirectional (BD) are some of the most common topologies [41].

Several different control laws have been investigated for CACC systems. Some studies proposed augmenting current ACC systems with a feed-forward term based on the information received from other vehicles (e.g. [24], [26]). Whereas, Desjardins and Chaib-draa [9] proposed a reinforced learning approach to improve system performance, Onieva *et al.* proposed a online fuzzy controller to adapt to uncertainties and Stanger and del Re [34] proposed an MPC-based approach which internalized the powertrain efficiency.

Increased fuel savings have been reported by studies [24], [28], [36] on CACC for heavy trucks and vans, when the clearance between vehicles on the platoon decreased, due to aerodynamic effects. Whereas, other studies [23], [34] have explicitly incorporated driver models and powertrain models to explicitly optimize fuel consumption.

Reduction of vehicle clearances can also increase road traffic throughput in 273% for 100% market penetration [35], under the assumption that vehicles can cruise with a 2 meters clearance. High market penetrations can also significantly influence flow characteristics, reducing remaining manual drivers influence on it and stop-and-go conditions [39].

Given the prospects in the optimization of both fuel consumption and road throughput, technical possibilities of decreasing the distance while maintaining vehicle safety should be further investigated. Van Willigen *et al.* [38] investigated a minimum safe headway time based on parameter uncertainties and system delays.

Safety boundaries can be easily violated by disturbances when vehicles cruise at such small clearances. One possible approach to avoid such violations is to design controllers with stability, performance and feasibility robustness with respect to such disturbances. Few studies have investigated robust control approaches for CACC systems. Corona *et al.* [8] proposed a Robust Hybrid Model Predictive Control approach to handle uncertainties in the piece-wise linear approximated powertrain and brake dynamics and Ploeg *et al.* [29] investigated mixed-sensitivity $\mathcal{H}_\infty$ synthesis to design a fault-tolerant CACC controller.

Besides technical factors, drivers and passengers must feel comfortable with small clearances and trust the CACC system. However, there are few studies on human factors of CACC system design [10]. Among these preliminary studies, [25] investigated the acceptance of sub-second headway time setups and concluded that test subjects were comfortable with the system operating under such condition.

III. Modeling

Assumption 1: The powertrain and brake dynamics of the controlled vehicle can be approximated by an inversible steady-state time-invariant model with no introduction of significant uncertainties to the system.

Assumption 1 was experimentally validated in [21]. Therefore, the powertrain and brake dynamics have been abstracted from the model, reducing its complexity while maintaining performance.

The proposed controller was designed to regulate the vehicle distance, velocity and acceleration considering only the (immediate) preceding vehicle. Therefore, a simplified kinematic model of both vehicles longitudinal dynamics is used and described in Definitions 1 and 2.

Definition 1: Let $p_i(t)$, $v_i(t)$ and $a_i(t)$ denote the position, velocity and acceleration of vehicle i, respectively. Then, the vehicle dynamics are represented by

$$\begin{aligned} \dot{p}_i(t) &= v_i(t) \\ \dot{v}_i(t) &= a_i(t) \end{aligned} \tag{1}$$

as shown in both vehicles of Figure 1.

Definition 2: Consider two adjacent vehicles on a platoon. Let the preceding vehicle states be denoted by subscript l, the ego vehicle be denoted by subscript e and $d(t) = p_l(t) - p_e(t)$ be the distance between these vehicles. The relative dynamics are

$$\begin{aligned} \dot{d} &= v_l(t) - v_e(t) \\ \ddot{d} &= a_l(t) - a_e(t). \end{aligned} \tag{2}$$

Let the system state be $x(t) = [d(t), v_l(t), v_e(t)]^T$ and the control input $u(t) = a_e(t)$. Then, the system from Definitions 1 and 2 can be written as a linear affine continuous system of the form

$$\dot{x}(t) = F_c x(t) + G_c u(t) + h_c(t) \tag{3}$$

where

$$F_c = \begin{bmatrix} 0 & 1 & -1 \\ 0 & 0 & 0 \\ 0 & 0 & 0 \end{bmatrix}, \quad G_c = \begin{bmatrix} 0 \\ 0 \\ 1 \end{bmatrix}, \quad h_c(t) = \begin{bmatrix} 0 \\ a_l(t) \\ 0 \end{bmatrix}. \quad (4)$$

This model assumes the preceding vehicle acceleration is constant and equal to the current acceleration. However, this assumption does not hold if this model is used for prediction of future states, since the preceding vehicle acceleration varies with time.

Assumption 2: There exists an upper bound j_l^{max} to the preceding vehicle jerk $j_l(t)$, such that

$$\forall t > 0 : |j_l(t)| \leq j_l^{max}. \quad (5)$$

From Assumption 2, the prediction of the system state over a horizon τ can be described as a uncertain affine linear system, described by

$$\dot{x}(t+\tau \mid t) = F_c x(t+\tau \mid t) + G_c u(t+\tau) + h_c(t) + W_c w(t+\tau), \quad (6)$$

where $w(t) \in \mathbb{R}$ is the uncertain variable (normalized jerk), such that $|w(t)| \leq 1$, and

$$W_c = \begin{bmatrix} 0 \\ \tau j_l^{max} \\ 0 \end{bmatrix}. \quad (7)$$

It is assumed that the preceding vehicle acceleration is obtained through the V2V communication, the relative position are obtained through dedicated sensors and the relative speed is obtained by both. Notice in this case that the fusion of these sensors with V2V communication can improve the measurement accuracy.

IV. Platooning Safety and Comfort Considerations

This section is divided into three parts - the first defines the minimum safety distance between two vehicles, the second investigates its impact on small clearance assumptions and the third addresses the comfort and safety restrictions the system must satisfy.

A. Minimum Safety Distance

Most economical benefits from CACC systems are related to the assumption this technology will enable vehicles to drive very close to each other. Therefore, a worst-case representation of the minimum safety distance between vehicles enables the system to avoid compromising system safety and provides a lower bound to vehicle distances.

The minimum safety distance concept proposed in this paper focuses on the predecessor following topology, in which every vehicle is responsible for ensuring its safety with respect to its immediate preceding vehicle.

Assumption 3: The preceding vehicle will never decelerate more than its claimed maximum braking capacity.

Assumption 3 cannot be satisfied if the preceding vehicle is involved in a collision, and further investigation is required for the removal of the assumption.

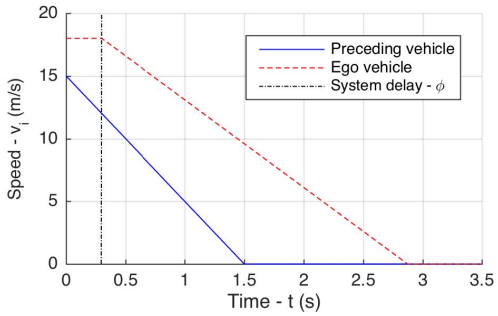

Fig. 2. Example of the vehicle velocity profiles in an emergency situation of Definition 3, where the preceding vehicle cruises at $15m/s$ with $a_l^b = 10m/s^2$ braking capacity and an ego vehicle cruises at $18m/s$ with $a_e^b = 7m/s^2$ braking capacity.

Definition 3: Let ϕ be the sum of worst-case delays from communication, processing and actuation. Consider the system model from Definition 2 where both preceding and ego vehicles brake at their maximum braking capacity a_l^b and a_e^b at time t and $t+\phi$, respectively, until both reach complete stop. $d_{safe}(t) \in \mathbb{R}$ is said to be the minimum safety distance if

$$d(t) \geq d_{safe}(t) \Rightarrow \forall \epsilon \in \mathbb{R}_{\geq 0}.\, d(t+\epsilon) \geq 0 \quad (8)$$

with

$$\dot{v}_l(\tau) = a_l(\tau) = \begin{cases} -a_l^b, & 0 \leq \tau - t \leq \dfrac{v_l(t)}{a_l^b} \\ 0, & otherwise, \end{cases} \quad (9)$$

and

$$\dot{v}_e(\tau) = a_e(\tau) = \begin{cases} -a_e^b, & 0 \leq \tau - t - \phi \leq \dfrac{v_e(t)}{a_e^b} \\ 0, & otherwise. \end{cases} \quad (10)$$

Therefore, d_{safe} is given by

$$d_{safe} = \min_d d \quad s.t.\ d + \min_{t \leq \epsilon \leq \infty} \left\{ \int_t^{\epsilon} v_l(\tau) - v_e(\tau) d\tau \right\} \geq 0. \quad (11)$$

Definition 3 requires the knowledge of the current maximum braking capacity which is inherently dependent on the road-tire friction coefficient. This coefficient can be estimated based on the longitudinal tire slip [13], lateral tire slip [15] or based on the steering self aligning moment [17].

Figure 2 shows an example of the vehicles' velocity profiles for Definition 3.

Lemma 1: d_{safe} has a closed form solution

$$d_{safe} = \begin{cases} d_{safe}^{lo}, & \epsilon \in [t+\phi, t+t_f^{min}) \\ \max\left(0, d_{safe}^{ub}\right), & otherwise \end{cases} \quad (12)$$

where

$$\epsilon^* = \frac{v_e(t) - v_l(t) + a_e^b \phi}{a_e^b - a_l^b}$$

$$d_{safe}^{ub} = v_e(t)\phi + \frac{v_e(t)^2}{2a_e^b} - \frac{v_l(t)^2}{2a_l^b}$$

$$d_{safe}^{lo} = (v_e(t) - v_l(t))\epsilon^* - (a_e^b - a_l^b)\frac{\epsilon^{*2}}{2} + a_e^b \frac{\phi^2}{2}. \quad (13)$$

Proof: Let $t_f^e = \phi + v_e(t)/a_e^b$, $t_f^l = v_l(t)/a_l^b$, $t_f^{min} = \min\left(t_f^e, t_f^l\right)$ and $t_f^{max} = \max\left(t_f^e, t_f^l\right)$ for brevity. Since (11) shows a linear minimization with a lower bound,

$$d_{safe} = \max_{t \le \epsilon \le \infty} \left\{ \int_t^{\epsilon} v_e(\tau) - v_l(\tau) d\tau \right\}. \tag{14}$$

Both $v_e(t)$ and $v_l(t)$ are continuous piecewise linear functions, therefore, $\delta v(t) = v_e(t) - v_l(t)$ is also piecewise linear and

$$J_{dist}(\epsilon) = \int_t^{\epsilon} \delta v(\tau) d\tau \tag{15}$$

is a twice-differentiable piecewise quadratic function. It is also worth noting that

$$J_{dist}(\epsilon) = J_{dist}(\infty), \quad \forall \epsilon > t + t_f^{max}. \tag{16}$$

Since the maximization problem is not always concave, but has a small number of possible optimal solutions, the optimization can be expressed analytically through enumeration [19]. There exists three possible positions for the constrained global maximum: lower optimization bound, upper optimization bound and a local maximum inside the feasible set. The lower bound case can be trivially obtained as $d_{safe}^{lb} = 0$, while the upper bound case is

$$\begin{aligned} d_{safe}^{ub} &= J_{dist}(\infty) \\ &= \int_t^{\infty} \delta v(\tau) d\tau \\ &= v_e(t)\phi + \frac{v_e(t)^2}{2a_e^b} - \frac{v_l(t)^2}{2a_l^b}. \end{aligned} \tag{17}$$

The latter case requires the enumeration of all $\{\epsilon \mid \dot{J}_{dist}(\epsilon) = 0, \ \ddot{J}_{dist}(\epsilon) < 0\}$. The Hessian of $J_{dist}(\epsilon)$ can be expressed as

$$\ddot{J}_{dist}(\epsilon) = \begin{cases} a_l^b, & 0 \le \epsilon - t < \phi \\ a_l^b - a_e^b, & \phi \le \epsilon - t < t_f^{min} \\ a_l^b, & t_f^{min} \le \epsilon - t < t_f^{max}, \ t_f^l > t_f^e \\ -a_e^b, & t_f^{min} \le \epsilon - t < t_f^{max}, \ t_f^e >= t_f^l \\ 0, & t_f^{max} < \epsilon - t \end{cases} \tag{18}$$

which it is negative only for $\epsilon \in \{\epsilon \mid \epsilon \in [t+\phi, t+t_f^{min}), \ a_e^b > a_l^b\}$ or $\epsilon \in \{\epsilon \mid \epsilon \in [t + t_f^{min}, t + t_f^{max}), \ t_f^e >= t_f^l\}$. However, $\dot{J}_{dist}(\epsilon) \neq 0 \ \forall \epsilon \in [t + t_f^{min}, t + t_f^{max})$, therefore $\ddot{J}_{dist}(\epsilon)$ has a local maximum in ϵ^* only if $a_e^b > a_l^b$ and $\dot{J}_{dist}(\epsilon^*) = 0$, which can be expanded as

$$v_e(t) - a_e^b(\epsilon^* - \phi) = v_l(t) - a_l^b \epsilon^* \tag{19}$$

and results

$$\epsilon^* = \frac{v_e(t) - v_l(t) + a_e^b \phi}{a_e^b - a_l^b} \iff \epsilon^* \in [t + \phi, t + t_f^{min}). \tag{20}$$

The local optima minimum safety distance can be expressed as

$$\begin{aligned} d_{safe}^{lo} &= J_{dist}(\epsilon^*) \\ &= \int_t^{\epsilon^*} \delta v(\tau) d\tau \\ &= (v_e(t) - v_l(t))\epsilon^* - (a_e^b - a_l^b)\frac{\epsilon^{*2}}{2} + a_e^b \frac{\phi^2}{2}. \end{aligned} \tag{21}$$

Finally d_{safe} is the enumeration of all previous possible maximums, which results in

$$d_{safe} = \begin{cases} d_{safe}^{lo}, & \epsilon \in [t + \phi, t + t_f^{min}) \\ \max\left(0, d_{safe}^{ub}\right), & otherwise. \end{cases} \tag{22}$$

■

The safety distance concept presented in Lemma 13 is conservative since it does not take into account any other vehicle besides the immediately preceding one. However, it is also the most robust since it guarantees not only the platoon safety, but also the safety of any of its contiguous subsets. It is also robust to unmodeled higher order dynamics, since it provides an upper bound for the minimum safety distances if the effective preceding vehicle velocity is higher than the modeled and the ego vehicle velocity is lower than the modeled. These conditions can be satisfied with a proper selection of ϕ and conservative values for the maximum brake capacity of the vehicles (over-estimating for the preceding vehicle and under-estimating for the ego vehicle).

B. Impact of Minimum Safety Distance on Cooperative Adaptive Cruise Control Performance

Consider both vehicle velocities are equal and in steady-state, $a_e^b = a_l^b = 9m/s^2$ and $\phi = 0.27s$ (approximately $150ms$ of actuation delay, $100ms$ of processing delay and $20ms$ of communication delay). The minimum safe distance is $9.72m$ for $v_e(t) = v_l(t) = 35m/s$ ($126km/h$) and $6.94m$ for $v_e(t) = v_l(t) = 25m/s$ ($90km/h$), as shown in Figure 3.

The minimum safety distance obtained is superior to the distances investigated in previous studies (such as [35] and [36]), in which vehicles operated down to $2m$ clearances at highway velocities. For the achievement of such clearances, the overall delay required for vehicles with similar braking capacity would be $80ms$ for $25m/s$ and $57ms$ for $35m/s$. The required delays are not consistent with the state-of-the-art actuators and wireless transmission systems, since current DSRC systems have a worst-case delay of $22ms$ on benchmarks [31] and braking systems take up to $100ms$ to achieve the commanded pressure. However, significant benefits can be delivered by CACC systems capable of operating near the minimum safety distance, since fuel savings can still be obtained at $10m$ clearances [28], [36].

Sorting the vehicles within the platoon from the least braking capacity (e.g. a heavy truck with a trailer) to the highest braking capacity (e.g. a sport car) would decrease the overall platoon clearance and maintain safety guarantees. However, such sorting would result in situations in which the vehicle with slowest braking response would become the platoon

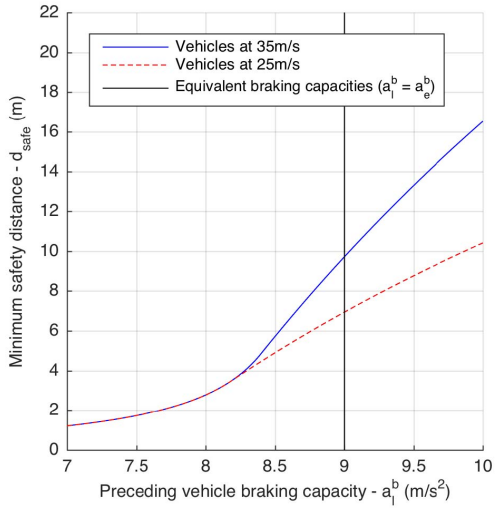

Fig. 3. Minimum distance in function of the preceding vehicle braking capacity for an ego vehicle braking capacity $a_e^b = 9m/s^2$ and both vehicles cruising at $35m/s$ (blue line) and $25m/s$ (red dashed line).

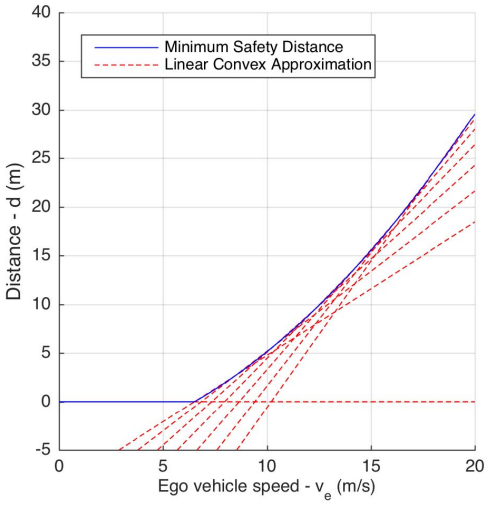

Fig. 4. Minimum safety distance constraint and its linear convex approximation for $v_l = 10m/s$, $a_e^b = 7m/s^2$ and $a_l^b = 10m/s^2$.

leader and be entitled of the mitigation of all forward external emergencies. Therefore, a trade-off between the minimization of the clearance inside a platoon and the robustness guarantees against external incidents indeed exists.

From (12), the minimum safety distance varies quadratically with both ego vehicle and preceding vehicle velocities. Thereafter, a constant distance CACC controller would be required to maintain the highest safety distance within the operating velocity range to ensure the vehicle safety. Likewise, a constant headway time CACC controller would be required to maintain the highest safety headway time within the operating velocity range. Thus, both of these approaches would result in higher clearances (and consequently higher fuel consumption) than the direct use of the minimum safety distance. Hence, this study focuses in the latter case, incorporating the minimum safety distance into the controller design through constraints, as it is presented in the next section.

C. Safety and Comfort Constraints

The following two factors must be taken into consideration when techniques for any type of vehicle control are investigated: vehicle must be safe at all times and its behavior must be comfortable whenever possible.

Safety constraints must be met at all times, regardless of system disturbances, while comfort must be met whenever it does not compromise the safety of the vehicle. Therefore, four constraint sets were defined:

- Minimum safety distance set *(safety)* - Ensures the concept shown in Section IV-A is satisfied;
- time-to-collision set *(comfort)* - Ensures a minimum time required for a collision to occur between the preceding and ego vehicle if velocities are kept constant;
- Road velocity limit set *(safety)* - Ensures the vehicle does not exceed the maximum velocity or moves backwards,
- Acceleration limits set *(comfort)* - Ensures the acceleration is maintained within comfortable levels whenever possible.

The minimum safety distance set enforces the minimum distance to the preceding vehicle, as defined in (12). This constraint is nonlinear, but convex on $d(t)$ and $v_e(t)$ and non-convex on uncontrollable $v_l(t)$.

Let $f\left(v_e(t), v_l(t)\right) : \mathbb{R}^2 \to \mathbb{R}$ define the minimum safety distance relation d_{safe} for a given set of parameters ϕ, a_e^b and a_l^b, such that $-d(t) + f\left(v_e(t), v_l(t)\right) \leq 0$ defines its constraint. Based on Assumption 2, the future preceding vehicle velocity satisfies

$$v_l(t+\tau) \geq v_l(t) + \tau a_l(t) - \frac{\tau^2}{2} j_l^{max} \tag{23}$$

and the minimum safety distance satisfies

$$\begin{aligned} &f\left(v_e(t+\tau), v_l(t+\tau)\right) \\ &\quad \leq f\left(v_e(t+\tau), v_l(t) + \tau a_l(t) - \frac{\tau^2}{2} j_l^{max}\right) \\ &\quad = g\left(t+\tau, v_e(t+\tau)\right). \end{aligned} \tag{24}$$

Through this approximation, the resulting function g is a convex function that can be conservatively represented by a set of linear constraints, as shown in Figure 4.

This set of linear constraints consists of one constraint for the linear region

$$-d(t) \leq 0, \quad \forall v_e(t) \in [0, v_{min}] \tag{25}$$

where

$$v_{min} = \sqrt{\frac{v_l(t)^2 a_e^b}{a_l^b}} \tag{26}$$

and seven constraints between v_{min} and road velocity limit v_{max} for the nonlinear region given by Taylor approximation of function g at a given point $p_i = v_{min} + i(v_{max} - v_{min})/7, \forall i \in [0, 7]$

$$-d(t) + g(t, p_i) + \frac{g(t, p_{i+1}) - g(t, p_i)}{p_{i+1} - p_i}(v_e(t) - p_i) \leq 0. \tag{27}$$

Since this constraint is dependent on t, it must be defined once for each step where the system is evaluated. The set will be compactly denoted as

$$-\mathbb{1}_8 d(t) + f(t) + g(t)v_e(t) \leq 0 \tag{28}$$

where $\mathbb{1}_i$ is an one-column vector of size i.

The time-to-collision constraint avoids fast approximations to the preceding vehicle that might be uncomfortable to passengers.

Definition 4: Let time-to-collision $t_c(t)$ be the instantaneous time required for a collision to occur between the preceding and ego vehicle if no vehicles varies its velocity.

$$\begin{aligned} t_c(t) = \min\ & \tau \\ s.t.\ & d(\tau) = 0 \\ & \dot{d}(\tau) = v_l(t) - v_e(t) \\ & \tau \geq 0 \end{aligned} \tag{29}$$

which has a closed form solution

$$t_c(t) = \max\left(\frac{d(t)}{v_e(t) - v_l(t)}, 0\right). \tag{30}$$

Assumption 4: A minimum value of t_c, denoted by $t_{c,min}$, is considered comfortable by the driver and passengers of the ego vehicle.

The time-to-collision constraint based on Definition 4 and Assumption 4 is

$$t_{c,min} \leq t_c(t) = \frac{d(t)}{v_e(t) - v_l(t)}, \quad \forall t \in \mathbb{R} \tag{31}$$

which can be rewritten in the canonical form as

$$-d(t) + t_{c,min}(v_e(t) - v_l(t)) \leq 0. \tag{32}$$

The road velocity limit constraint set avoids the vehicle to exceed the maximum velocity on the road. Therefore, it can be trivially defined as

$$0 \leq v_e(t) \leq v_{max}. \tag{33}$$

Finally, the acceleration constraint set limits the controller acceleration to what is achievable given the current friction limits and brake distribution and limits the vehicle acceleration to a comfortable region whenever possible. For the first role, the constraint can be defined in the canonical form as

$$-a_e(t) \leq -a_e^b \tag{34}$$

whereas for the second, a slack variable $s_a(t)$ will be introduced for the creation of a *soft* constraint, which results

$$a_{min} \leq a_e(t) + s_a(t) \leq a_{max} \tag{35}$$

where a_{min} and a_{max} define the comfortable acceleration limits and

$$x(t) \leftarrow [x^T(t), s_a(t)]^T \tag{36}$$

for optimization purposes.

All constraints will be represented by their generic form $A(t)x(t) + Bu(t) + c(t) \leq 0$ for brevity, where

$$A(t) = \begin{bmatrix} 0 & 0 & -1 & 0 \\ 0 & 0 & 1 & 0 \\ -1 & t_{c,min} & -t_{c,min} & 0 \\ 0 & 0 & 0 & 0 \\ 0 & 0 & 0 & -1 \\ 0 & 0 & 0 & 1 \\ -\mathbb{1}_8 & 0 & g(t) & 0 \end{bmatrix}$$

$$B = \begin{bmatrix} 0 \\ 0 \\ 0 \\ -1 \\ -1 \\ 1 \\ 0 \end{bmatrix} \quad c(t) = \begin{bmatrix} 0 \\ v_{max} \\ 0 \\ -a_e^b \\ -a_{min} \\ a_{max} \\ -f(t) \end{bmatrix}. \tag{37}$$

V. Proposed Controller

This section addresses the formulation of the $l\infty$-norm robust optimal control based on the min-max approach and presents the pre-stabilizing nil-potent controller concept.

A. $l\infty$-Norm Robust Optimal Control Formulation

MPC problems are often expressed in function of an $l2$-norm functional, similar to LQR formulation. However, it can only incorporate polytopic uncertainties by explicitly enumerating the uncertain polytope vertexes [33] which increases the optimization problem complexity exponentially and is not suitable for real-time applications. $l1$-norm and $l\infty$-norm-based MPC formulations were proposed to address this curse of dimensionality, in these optimization problems robustness can be achieved through the explicit maximization of the uncertainty terms [20]. It increases the optimization complexity linearly, instead of exponentially for the enumeration approach. $l1$-norm MPC often results in the sparsest solution [11], resulting in controllers with a bang-bang behavior which would violate comfort requirements. For this reason an $l\infty$-norm MPC formulation was chosen for this controller design.

Let $F \in \mathbb{R}^{N_x \times N_x}$, $G \in \mathbb{R}^{N_x \times N_u}$, $W \in \mathbb{N} \times \mathbb{N}$ and $h \in \mathbb{R}^{N_x}$ represent the discrete time dynamics counterpart of F_c, G_c, W_c and h_c, respectively, calculated using the exact discretization method with sampling time T_s, $x_k = x(t + kT_s)$, $u_k = u(t + kT_s)$, $A_k = A(t + kT_s)$, $B_k = B$ and $c_k = c(t + kT_s)$. Then, the optimization problem of an $l\infty$-norm optimal receding horizon control formulation [7] is given by

$$\begin{aligned} J^*(x_0) = \min_{x,u} & \sum_{k=0}^{T-1} ||Qx_k||_\infty + ||Ru_k||_\infty + ||P_\infty x_T||_\infty \\ s.t.\ & x_{k+1} = Fx_k + Gu_k + h + Ww_k \\ & A_k x_k + B_k u_k + c_k \leq 0 \end{aligned} \tag{38}$$

where the range of k has been omitted for brevity, T is the prediction horizon, $A_k \in \mathbb{R}^{N_c \times N_x}, \forall k \in [0, T]$, $B_k \in \mathbb{R}^{N_c \times N_u}, \forall k \in [0, T]$ and $c_k \in \mathbb{R}^{N_c}, \forall k \in [0, T]$ define a polytopic inequality constraint, $Q \in \mathbb{R}^{N_w x \times N_x}$ and $R \in$

$\mathbb{R}^{N_w c \times N_u}$ are full lower rank real matrices and $P_\infty \in \mathbb{R}^{N_p \times N_x}$ is the cost matrix of the infinite horizon unconstrained $l\infty$-norm problem

$$||P_\infty x_0||_\infty = \min_{x,u} \sum_{k=0}^{\infty} ||Qx_k||_\infty + ||Ru_k||_\infty$$
$$s.t.\ x_{k+1} = Fx_k + Gu_k + h. \tag{39}$$

The problem in (38) can be represented as a Linear Programming (LP) problem based on the relaxation of the $l\infty$-norm cost functional through

$$||v||_\infty = \min_{\epsilon} \epsilon$$
$$s.t.\ \forall i : v^{(i)} \le \epsilon$$
$$\forall i : -v^{(i)} \le \epsilon \tag{40}$$

for a given vector v, where $v^{(i)}$ is the i-th row of vector v and ϵ is a auxiliary optimization variable with optimal value $\epsilon^* = ||v||_\infty$ [5]. Therefore, with auxiliary variables $\epsilon_k^x \in \mathbb{R},\ \forall k \in [0, T]$ and $\epsilon_k^u \in \mathbb{R},\ \forall k \in [0, T-1]$, (38) is relaxed as

$$\begin{aligned} J^*(x_0) = \min_{x,u,\epsilon^x,\epsilon^u}\ & \epsilon_T^x + \sum_{k=0}^{T-1} \epsilon_k^x + \epsilon_k^u \\ s.t.\ & x_{k+1} = Fx_k + Gu_k + h + Ww_k \\ & A_k x_k + B_k u_k + c_k \le 0 \\ & Q_i x_k \le \epsilon_k^x \\ & -Q_i x_k \le \epsilon_k^x \\ & R_i u_k \le \epsilon_k^u \\ & -R_i u_k \le \epsilon_k^u \\ & (P_\infty)_i x_T \le \epsilon_T^x \\ & -(P_\infty)_i x_T \le \epsilon_T^x \end{aligned} \tag{41}$$

where Q_i, R_i and $(P_\infty)_i$ are the i-th row of matrices Q, R and P_∞, respectively.

The system should remain constrained and stable under any possible value of $w \in \mathcal{W}$, where $\mathcal{W} = \{w \mid w \in \mathbb{R}^N,\ ||w||_\infty \le 1\}$. Therefore, let $\bar{x}_k \in \mathbb{R}^{N_x}$ be the process state without disturbances. The representation of both x_k and $\bar{x}_k$ in respect to a known current state $x_0 = \bar{x}_0$ results in

$$x_k = F^{k-1}x_0 + \sum_{i=0}^{k-1} F^{k-i-1}(Gu_i + h) + \sum_{i=0}^{k-1} F^{k-i-1} W w_i,$$
$$\bar{x}_k = F^{k-1}x_0 + \sum_{i=0}^{k-1} F^{k-i-1}(Gu_i + h) \tag{42}$$

and defining $\bar{W}_i = F^{i-1}W$ for brevity, the relation between x_k and $\bar{x}_k$ is

$$x_k = \bar{x}_k + \sum_{i=0}^{k-1} \bar{W}_{k-i} w_i. \tag{43}$$

The substitution of (43) in (41) yields

$$\begin{aligned} J^*(x_0) = \min_{x,u,\epsilon^x,\epsilon^u}\ & \epsilon_T^x + \sum_{k=0}^{T-1} \epsilon_k^x + \epsilon_k^u \\ s.t.\ & \bar{x}_{k+1} = Fx_k + Gu_k + h \\ & A_k \bar{x}_k + B_k u_k + c_k + A \sum_{i=0}^{k-1} \bar{W}_{k-i} w_i \le 0 \\ & Q_i \bar{x}_k + Q_i \sum_{j=0}^{k-1} \bar{W}_{k-j} w_j \le \epsilon_k^x \\ & -Q_i \bar{x}_k - Q_i \sum_{j=0}^{k-1} \bar{W}_{k-j} w_j \le \epsilon_k^x \\ & R_i u_k \le \epsilon_k^u \\ & -R_i u_k \le \epsilon_k^u \\ & (P_\infty)_i \bar{x}_T + (P_\infty)_i \sum_{j=0}^{T-1} \bar{W}_{k-j} w_j \le \epsilon_T^x \\ & -(P_\infty)_i \bar{x}_T - (P_\infty)_i \sum_{j=0}^{T-1} \bar{W}_{k-j} w_j \le \epsilon_T^x \end{aligned} \tag{44}$$

where all uncertain variables are only present in polytopic constraints.

Theorem 1: Let $p \in \mathbb{R}_{+\infty}$, $p^* \in \mathbb{R}_{+\infty}$, $q \in \mathbb{R}^N$ and $x \in \mathcal{X}$ where $\mathcal{X} = \{x \mid x \in \mathbb{R}^N,\ ||x||_p \le 1\}$ and $1/p + 1/p^* = 1$ then

$$q^T x \le \max_{||x||_p \le 1} q^T x = ||q||_{p^*}. \tag{45}$$

Proof: Adapted from [6]. If both q and x are finite, there is an upper bound to $q^T x$ given by HÃlder's inequality as

$$q^T x \le ||x||_p ||q||_{p^*} \tag{46}$$

by definition, $||x||_p \le 1$, therefore

$$q^T x \le ||x||_p ||q||_{p^*} \le ||q||_{p^*} \tag{47}$$

results in an upper bound to the constrained maximization

$$J(q) = \max_{||x||_p \le 1} q^T x = ||q||_{p^*}. \tag{48}$$

□

Let $|M|$ be the element-wise modulus of a given matrix M. Through Theorem 1, it follows that

$$Mw \le \max_{||w||_\infty \le 1} Mw = |M| \mathbb{1}_{N_w} \tag{49}$$

and the robust polytopic constraint from (44) is

$$A_k \bar{x}_k + B_k u_k + c_k + \sum_{i=0}^{k-1} |A_k \bar{W}_{k-i}| \mathbb{1}_{N_w} \le 0. \tag{50}$$

Analogously

$$\begin{aligned} Q_i\bar{x}_k + \sum_{i=0}^{k-1}|Q_i\bar{W}_{k-i}|\mathbb{1}_{N_w} &\leq \epsilon_k^x \\ -Q_i\bar{x}_k + \sum_{i=0}^{k-1}|Q_i\bar{W}_{k-i}|\mathbb{1}_{N_w} &\leq \epsilon_k^x \\ (P_\infty)_i\bar{x}_T + \sum_{j=0}^{T-1}|(P_\infty)_i\bar{W}_{k-j}|\mathbb{1}_{N_w} &\leq \epsilon_T^x \\ -(P_\infty)_i\bar{x}_T + \sum_{j=0}^{T-1}|(P_\infty)_i\bar{W}_{k-j}|\mathbb{1}_{N_w} &\leq \epsilon_T^x. \end{aligned} \tag{51}$$

The robust counterpart of the optimization problem from (44) based on (50) and (51) is

$$\begin{aligned} \bar{J}^*(x_0) = \min_{x,u,\epsilon^x,\epsilon^u}\ & \epsilon_T^x + \sum_{k=0}^{T-1}\epsilon_k^x + \epsilon_k^u \\ s.t.\ & \bar{x}_{k+1} = Fx_k + Gu_k + h \\ & A_k\bar{x}_k + B_ku_k + c_k + \Phi_A(k) \leq 0 \\ & Q_i\bar{x}_k + \Phi_Q(k) \leq \epsilon_k^x \\ & -Q_i\bar{x}_k + \Phi_Q(k) \leq \epsilon_k^x \\ & R_iu_k \leq \epsilon_k^u \\ & -R_iu_k \leq \epsilon_k^u \\ & (P_\infty)_i\bar{x}_T + \Phi_P(T) \leq \epsilon_T^x \\ & -(P_\infty)_i\bar{x}_T + \Phi_P(T) \leq \epsilon_T^x \end{aligned} \tag{52}$$

such that $\bar{J}^*(x_0) \geq J^*(x_0)$ and where $\Phi_A(k) = \sum_{i=0}^{k-1}|A_k\bar{W}_{k-i}|\mathbb{1}_{N_w}$, $\Phi_Q(k) = \sum_{i=0}^{k-1}|Q_i\bar{W}_{k-i}|\mathbb{1}_{N_w}$ and $\Phi_P(k) = \sum_{j=0}^{k-1}|(P_\infty)_i\bar{W}_{k-j}|\mathbb{1}_{N_w}$.

B. Pre-Stabilizing Nil-Potent Controller

Due to the disturbance modeled in the system, the formulation presented in (52) has the following disadvantage: the functional cost $\lim_{T\to\infty}\bar{J}^* \to \infty$ and the feasible set $\mathcal{C}_k = \{x_k, u_k \mid Ax_k + Bu_k + \bar{c}_k \leq 0\}$ becomes empty as $k \to \infty$ if the open-loop system is unstable or marginally stable. A possible approach for the mitigation of such an effect is the use of a nil-potent controller [3].

Definition 5: Let $x_k \in \mathbb{R}^{N_x}$ be the states and $u_k \in \mathbb{R}^{N_u}$ the control inputs of a system defined by $F \in \mathbb{R}^{N_x\times N_x}$, $G \in \mathbb{R}^{N_x\times N_u}$, such that $x_{k+1} = Fx_k + Gu_k$. A controller $K_0 \in \mathbb{R}^{N_u\times N_x}$ is an i-th order nil-potent controller if

$$(F - GK_0)^n = \mathbb{O}_{N_x}, \quad n \in \mathbb{I},\ n > i \tag{53}$$

where $\mathbb{O}_j$ is a zero column vector of size j.

Let $u_k = -K_0x_k + v_k$ and v_k be the new control input. The system pre-stabilized by an n-th order nil-potent controller is

$$\bar{x}_{k+1} = (F - GK_0)\bar{x}_k + Gv_k + h \tag{54}$$

and, given the results from (43), the system model with disturbances is written as

$$x_k = \bar{x}_k + \sum_{i=1}^{\min(k,n)}\bar{W}_iw_{k-i} \tag{55}$$

since

$$\bar{W}_i = \mathbb{O}_{N_x}, \quad \forall i > n. \tag{56}$$

Based on (54), (55) and (52), the pre-stabilized robust $l\infty$-norm optimal control problem, $\bar{J}^*_{np}(x_0)$ is

$$\begin{aligned} \bar{J}^*_{np}(x_0) = \min_{x,u,\epsilon^x,\epsilon^u}\ & \epsilon_T^x + \sum_{k=0}^{T-1}\epsilon_k^x + \epsilon_k^u \\ s.t.\ & \bar{x}_{k+1} = \widetilde{F}x_k + Gv_k + h \\ & \widetilde{A}_k\bar{x}_k + B_kv_k + c_k + \Phi_A(k) \leq 0 \\ & Q_i\bar{x}_k + \Phi_Q(k) \leq \epsilon_k^x \\ & -Q_i\bar{x}_k + \Phi_Q(k) \leq \epsilon_k^x \\ & -R_iK_0x_k + R_iv_k \leq \epsilon_k^u \\ & R_iK_0x_k - R_iv_k \leq \epsilon_k^u \\ & (P_\infty)_i\bar{x}_T + \Phi_P(T) \leq \epsilon_T^x \\ & -(P_\infty)_i\bar{x}_T + \Phi_P(T) \leq \epsilon_T^x \end{aligned} \tag{57}$$

where $\widetilde{F} = F - GK_0$ and $\widetilde{A}_k = A_k - B_kK_0$.

In this new form, $\mathcal{C}_k \geq \mathcal{C}_n, \forall k \in [0, T]$. Therefore, the feasible set converges to a smaller robust set given by $\mathcal{C}_n$ instead of becoming empty as $k \to \infty$.

VI. Controller Validation

This section is divided into two parts. The first describes the simulation framework developed for the validation of the control law and the second reports the simulation results for both robust and nominal controllers.

A. Simulation Framework

A simulation framework for multiple communicating vehicles was developed for the validation of the proposed controller based on the Robotic Operating System (ROS) [30]. It consists of five different processes:

1) Vehicle dynamics process - simulates longitudinal and lateral vehicle dynamics and provides noise for state measurements;
2) DSRC communication process - provides realistic delays and packet losses for V2V communication;
3) Vehicle behavior process - executes a predefined behavior profile of a vehicle;
4) Controller process - executes the proposed controller; and
5) Plotter process - displays the simulation results.

System architecture is shown in Figure 5, where blocks represent processes and arrows represent message passing

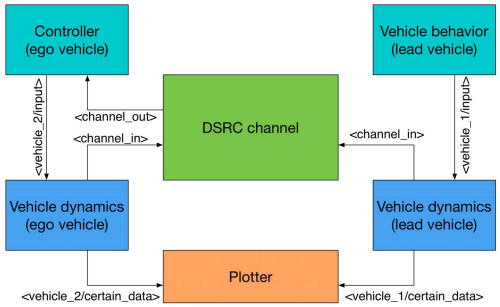

Fig. 5. Simulation framework architecture.

topics between the processes. Simulation assumed a constant $22ms$ communication delay and a constant 1% packet loss for all sent packets, based on the worst case scenario from [31]. An experiment with several follower vehicles was also performed and its results were omitted since they were comparable to a single leader-follower simulation. Thus the leader-follower results are presented. The simulated vehicle dynamics incorporates wheel inertial dynamics and a linear longitudinal slip model and does not incorporate powertrain and brake hydraulic dynamics. Noise was assumed Gaussian and independent for each state variable.

The controller was implemented using CVXGEN [22], a code-generation tool for small LP and QP solvers. The LP problem consisted of 80 optimization variables, 30 equality constraints and 248 inequality constraints for a 10 time-steps horizon ($0.5sec$ for $20Hz$ sampling frequency). The resulting optimization problem was solved in a minimum of $2ms$, a maximum of $37ms$ and on average $22ms$ on a $2.5Ghz$ i7-4980HQ with $16Gb$ of RAM. The infinite horizon unconstrained $l\infty$-norm optimal control problem was solved using the Multi-Parametric Toolbox (MPT) [16] based on the procedure outlined by [5].

B. Simulation Results

A short-term application of CACC systems focuses on highway driving scenarios. Therefore, the preceding vehicle velocity profile chosen, shown in Figure 6, starts at $15m/s$ $(54km/h)$ performing an on-ramp acceleration of $2m/s^2$ until it reaches $35m/s$ $(126km/h)$ at $t = 10s$. At this time, it maintains a constant velocity for $10s$, until $t = 20s$. It reduces velocity at $-1m/s^2$ until it reaches $25m/s$ $(90km/h)$ at $t = 30s$. At this time, it starts an emergency braking maneuver accelerating at $-10m/s^2$ until it reaches a complete stop at $t = 35s$. This profile enables the controller validation in both nominal and emergency cases. Additional simulation scenarios, and respective results, are available at https://github.com/cmasseraf/l_infinity_cacc.

Disturbances were added for the investigation of the controller robustness to unmodeled uncertainties. A step of amplitude $-3m$ was added to the distance between the vehicles at $t = 17s$ and a step of amplitude $-3m/s$ was added to the preceding vehicle velocity at $t = 22s$. The disturbance amplitudes were chosen to ensure violation of the minimum safety distance for both nominal and robust controllers.

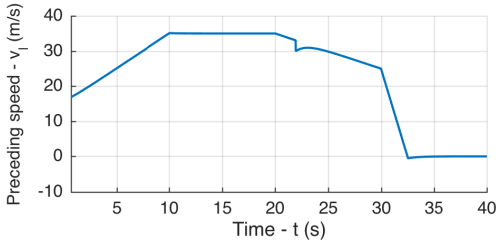

Fig. 6. Simulated preceding vehicle velocity profile.

TABLE I
INITIAL CONDITIONS AND VEHICLE PARAMETERS OF THE SIMULATION

Description	Symbol	Value	Unit
Initial distance	$d(0)$	15	m
Initial preceding vehicle velocity	$v_l(0)$	15	$\frac{m}{s}$
Initial ego vehicle velocity	$v_e(0)$	15	$\frac{m}{s}$
Maximum allowed velocity	v_{max}	40	$\frac{m}{s}$
Maximum acceleration	a_{max}	2.5	$\frac{m}{s^2}$
Minimum acceleration	a_{min}	-2.5	$\frac{m}{s^2}$
Minimum time-to-collision	$t_{c,min}$	2	s
Worst-case system delay	ϕ	0.3	s
Preceding vehicle maximum braking	a_l^b	10	$\frac{m}{s^2}$
Ego vehicle maximum braking	a_e^b	10	$\frac{m}{s^2}$
Operation frequency	–	20	Hz

The initial conditions and vehicle parameters used in the simulations are shown in Table I. Weighting matrices Q and R are given by

$$Q = \begin{bmatrix} 100 & 0 & 0 \\ 0 & 1 & -1 \end{bmatrix}, \quad R = \begin{bmatrix} 1 \end{bmatrix} \tag{58}$$

which were empirically tuned and the uncertainty matrix is given by $W = \begin{bmatrix} 0 & j_c^{max} T_s & 0 \end{bmatrix}^T$.

Simulation results for the nominal and robust controllers are shown in Figure 7. In Figures 7-(a) and 7-(d), the ego vehicle accelerates at the maximum allowed rate in order to catch up and reduce the distance to the vehicle ahead from time $t = 0s$ until $t = 4s$ in both controllers. Where they keep a constant clearance, close to the minimum safety distance, and the robust controller maintains a higher clearance until $t = 10s$.

At $t = 10s$, the preceding vehicle stops accelerating, so that the ego vehicle keeps a distance close to the minimum until the preceding vehicle starts to decelerate at $t = 20s$. Notice the performances of both control were similar until $t = 17s$, when a distance disturbance was introduced. The robust controller performs better on the recovery to a safe distance between the vehicles. When the preceding vehicle decelerates at $t = 20s$, the robust controller increases the robustness margin due to the prediction of a slower velocity ahead. The velocity disturbance at time $t = 22s$ caused an increase in the minimum safety distance, and both controllers responded in a similar manner.

The main advantage of the proposed robust approach is observed at the emergency braking maneuver at $t = 30s$, when it did not violate the minimum distance, unlike the nominal controller. This is due to the fact that the model internalized preceding vehicle acceleration uncertainties. It is also worth noting that distance and velocity uncertainties were not modeled since both controller had good disturbance rejection properties, as seen at $t = 17s$ and $t = 22$.

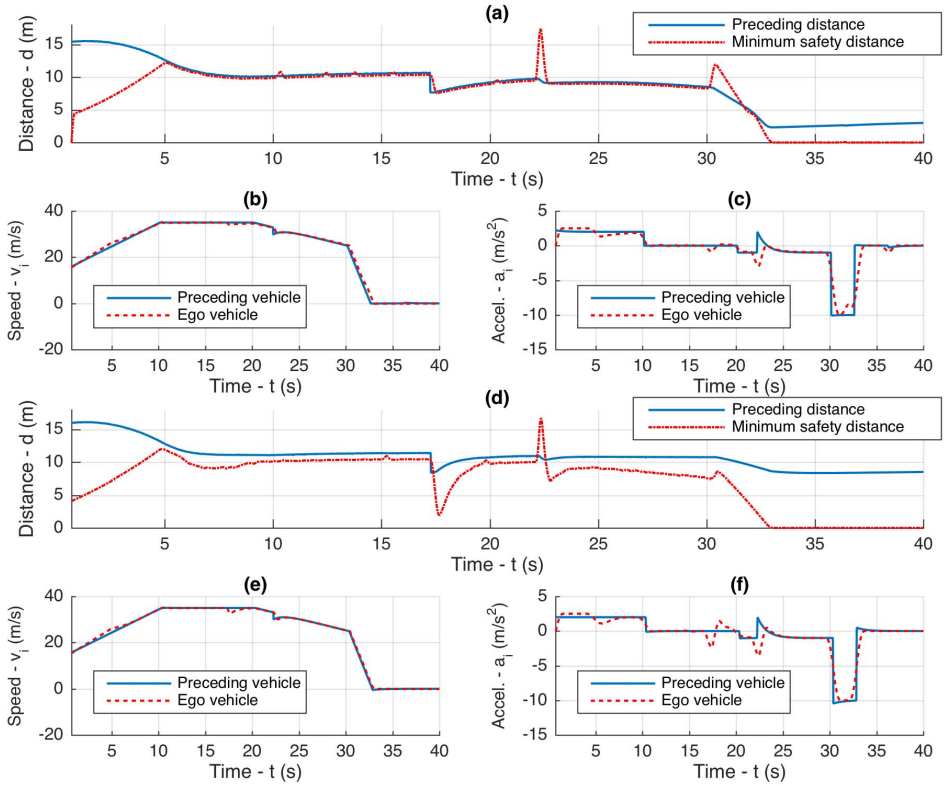

Fig. 7. Simulation results; (a) and (d) show the distance between both vehicles (blue line) and the minimum safety distance (red dashed line) for the nominal and robust $l\infty$-norm controllers, respectively; (b), (c), (e) and (f) show the preceding (blue line) and ego (red dashed line) vehicles velocity and acceleration profiles for the nominal and robust controllers, respectively

Both nominal and robust $l2$-norm-based MPC were also implemented for comparison. The nominal $l2$-norm controller results did not differ significantly from the nominal $l\infty$-norm-based approach. The robust $l2$-norm controller developed in [33] was not possible to be executed in the simulation environment used in this paper, since the min-max optimization problem of this approach needed more than $1s$ to be solved. Therefore, we could not guarantee the control system stability for this application.

VII. Conclusions

In this paper we have proposed an analytical formulation of the minimum safe distance between two vehicles and a robust $l\infty$-norm optimal controller for cooperative adaptive cruise control. The formulation provides a theoretical lower bound to vehicle clearance inside platoons and was used for the design of a controller capable of internalizing preceding vehicle acceleration uncertainties. It guarantees the ego vehicle will not collide with its preceding vehicle. It also maintains a sufficient small clearance to decrease fuel consumption. Validation simulations included on-ramp accelerations, small velocity variations and emergency braking situations, typical of highway driving. Results show that the robust controller operates correctly in both nominal and emergency scenarios. Overall, it achieved satisfactory distance and velocity tracking and increased the vehicle clearance during breaking to ensure vehicle safety, which resulted in a controller with intuitive behavior and robust to preceding vehicle actions. Since the resulting controller is piece-wise affine, including in regions where the constraints are not active, further investigation needs to be done on the string stability of this category of systems. Future work on the controller will also include reductions in acceleration disturbances due to measurement noises, incorporating the possibility of a preceding vehicle collision.

References

[1] T. A. Badgwell and S. J. Qin, *Model-Predictive Control in Practice*. London, U.K.: Springer, 2013, pp. 1–6. [Online]. Available: http://dx.doi.org/10.1007/978-1-4471-5102-9_8-1

[2] E. F. Belohoubek, "Radar control for automotive collision mitigation and headway spacing," *IEEE Trans. Veh. Technol.*, vol. 31, no. 2, pp. 89–99, May 1982.

[3] A. Bemporad and M. Morari, *Robust Model Predictive Control: A Survey*. London, U.K.: Springer, 1999, pp. 207–226. [Online]. Available: http://dx.doi.org/10.1007/BFb0109870

[4] M. Bergmans, H. Nijmeijer, and J. Ploeg, "A simulation model for I-GAME," Eindhoven Univ. Technol., Eindhoven, The Netherlands, Tech. Rep., 2014.[Online]. Available: https://pure.tue.nl/ws/files/3818590/605006965663895.pdf

[5] F. Borrelli, *Constrained Optimal Control of Linear and Hybrid Systems*, vol. 290. Berlin, Germany: Springer, 2003.

[6] S. Boyd and L. Vandenberghe, *Convex Optimization*. New York, NY, USA: Cambridge Univ. Press, 2004.

[7] F. J. Christophersen, "Optimal control and analysis for constrained piecewise affine systems," Ph.D. dissertation, Eidgenössische Technische Hochschule ETH Zürich, Zürich, Switzerland, 2006, p. 16807.

[8] D. Corona, I. Necoara, B. D. Schutter, and T. Van den Boom, "Robust hybrid MPC applied to the design of an adaptive cruise controller for a road vehicle," in *Proc. 45th IEEE Conf. Decision Control*, Dec. 2006, pp. 1721–1726.

[9] C. Desjardins and B. Chaib-draa, "Cooperative adaptive cruise control: A reinforcement learning approach," *IEEE Trans. Intell. Transp. Syst.*, vol. 12, no. 4, pp. 1248–1260, Dec. 2011.

[10] K. C. Dey *et al.*, "A review of communication, driver characteristics, and controls aspects of cooperative adaptive cruise control (CACC)," *IEEE Trans. Intell. Transp. Syst.*, vol. 17, no. 2, pp. 491–509, Feb. 2016.
[11] D. L. Donoho, "For most large underdetermined systems of linear equations the minimal 1-norm solution is also the sparsest solution," *Commun. Pure Appl. Math.*, vol. 59, no. 6, pp. 797–829, 2006.
[12] I. Gat, M. Benady, and A. Shashua, "A monocular vision advance warning system for the automotive aftermarket," Tech. Rep., 2005. [Online]. Available: http://dx.doi.org/10.4271/2005-01-1470
[13] F. Gustafsson, "Slip-based tire-road friction estimation," *Automatica*, vol. 33, no. 6, pp. 1087–1099, Jun. 1997.
[14] L. Güvenç *et al.*, "Cooperative adaptive cruise control implementation of team Mekar at the grand cooperative driving challenge," *IEEE Trans. Intell. Transp. Syst.*, vol. 13, no. 3, pp. 1062–1074, Sep. 2012.
[15] J.-O. Hahn, R. Rajamani, and L. Alexander, "GPS-based real-time identification of tire-road friction coefficient," *IEEE Trans. Control Syst. Technol.*, vol. 10, no. 3, pp. 331–343, May 2002.
[16] M. Herceg, M. Kvasnica, C. N. Jones, and M. Morari, "Multi-parametric toolbox 3.0," in *Proc. Eur. Control Conf.*, Zürich, Switzerland, Jul. 2013, pp. 502–510. [Online]. Available: http://control.ee.ethz.ch/~mpt
[17] Y.-H. J. Hsu, S. M. Laws, and J. C. Gerdes, "Estimation of tire slip angle and friction limits using steering torque," *IEEE Trans. Control Syst. Technol.*, vol. 18, no. 4, pp. 896–907, Jul. 2010.
[18] D. Jiang and L. Delgrossi, "IEEE 802.11p: Towards an international standard for wireless access in vehicular environments," in *Proc. Veh. Technol. Conf. VTC Spring*, May 2008, pp. 2036–2040.
[19] J. Löfberg, "Minimax approaches to robust model predictive control," Ph.D. dissertation, Autom. Control, Inst. Technol., Linköping Univ., Linköping, Sweden, 2003.
[20] J. Löberg, "Automatic robust convex programming," *Optim. Methods Softw.*, vol. 27, no. 1, pp. 115–129, 2012.
[21] C. M. Filho, D. F. Wolf, V. Grassi, and F. S. Osorio, "Longitudinal and lateral control for autonomous ground vehicles," in *Proc. Intell. Veh. Symp.*, Jun. 2014, pp. 588–593.
[22] J. Mattingley and S. Boyd, "CVXGEN: A code generator for embedded convex optimization," *Optim. Eng.*, vol. 13, no. 1, pp. 1–27, 2012.
[23] D. Moser, H. Waschl, H. Kirchsteiger, R. Schmied, and L. del Re, "Cooperative adaptive cruise control applying stochastic linear model predictive control strategies," in *Proc. Eur. Control Conf. (ECC)*, 2015, pp. 3383–3388.
[24] G. Naus, R. Vugts, J. Ploeg, R. van de Molengraft, and M. Steinbuch, "Cooperative adaptive cruise control, design and experiments," in *Proc. Amer. Control Conf.*, 2010, pp. 6145–6150.
[25] C. Nowakowski, J. O'Connell, S. E. Shladover, and S. Cody, "Cooperative adaptive cruise control: Driver acceptance of following gap settings less than one second," *Proc. Human Factors Ergonom. Soc. Annu. Meeting*, vol. 54, no. 24, pp. 2033–2037, 2010.
[26] S. Öncü, J. Ploeg, N. van de Wouw, and H. Nijmeijer, "Cooperative adaptive cruise control: Network-aware analysis of string stability," *IEEE Trans. Intell. Transp. Syst.*, vol. 15, no. 4, pp. 1527–1537, Aug. 2014.
[27] A. A. Peters, R. H. Middleton, and O. Mason, "Leader tracking in homogeneous vehicle platoons with broadcast delays," *Automatica*, vol. 50, no. 1, pp. 64–74, 2014.
[28] J. Ploeg, A. F. Serrarens, and G. J. Heijenk, "Connect & drive: Design and evaluation of cooperative adaptive cruise control for congestion reduction," *J. Modern Transp.*, vol. 19, no. 3, pp. 207–213, 2011.
[29] J. Ploeg, N. van de Wouw, and H. Nijmeijer, "Fault tolerance of cooperative vehicle platoons subject to communication delay," *IFAC-PapersOnLine*, vol. 48, no. 12, pp. 352–357, 2015.
[30] M. Quigley *et al.*, "ROS: An open-source robot operating system," in *ICRA Workshop Open Sour. Softw.*, 2009.
[31] A. Rauch, F. Klanner, and K. Dietmayer, "Analysis of v2x communication parameters for the development of a fusion architecture for cooperative perception systems," in *Proc. 4th Intell. Veh. Symp.*, Jun. 2011, pp. 685–690.
[32] J. Rawlings, E. Meadows, and K. Muske, "Nonlinear model predictive control: A tutorial and survey," in *Proc. Adv. Control Chem. Processes*, 1994, pp. 203–214.
[33] P. O. M. Scokaert and D. Q. Mayne, "Min-max feedback model predictive control for constrained linear systems," *IEEE Trans. Autom. Control*, vol. 43, no. 8, pp. 1136–1142, Aug. 1998.
[34] T. Stanger and L. del Re, "A model predictive cooperative adaptive cruise control approach," in *Proc. Amer. Control Conf. (ACC)*, Jun. 2013, pp. 1374–1379.
[35] P. Tientrakool, Y.-C. Ho, and N. F. Maxemchuk, "Highway capacity benefits from using vehicle-to-vehicle communication and sensors for collision avoidance," in *Proc. Veh. Technol. Conf. (VTC Fall)*, Sep. 2011, pp. 1–5.
[36] S. Tsugawa, "Results and issues of an automated truck platoon within the energy ITS project," in *Proc. Intell. Veh. Symp.*, Jun. 2014, pp. 642–647.
[37] B. van Arem, C. J. G. van Driel, and R. Visser, "The impact of cooperative adaptive cruise control on traffic-flow characteristics," *IEEE Trans. Intell. Transp. Syst.*, vol. 7, no. 4, pp. 429–436, Dec. 2006.
[38] W. van Willigen, L. Kester, E. van Nunen, and E. Haasdijk, "Safety in the face of uncertainty," *Int. J. Intell. Transp. Syst. Res.*, vol. 13, no. 2, pp. 95–106, 2015.
[39] M. Wang, W. Daamen, S. P. Hoogendoorn, and B. van Arem, "Cooperative car-following control: Distributed algorithm and impact on moving jam features," *IEEE Trans. Intell. Transp. Syst.*, vol. 17, no. 5, pp. 1459–1471, May 2016.
[40] Q. Xu, T. Mak, J. Ko, and R. Sengupta, "Vehicle-to-vehicle safety messaging in DSRC," in *Proc. 1st ACM Int. Workshop Veh. Ad Hoc Netw.*, 2004, pp. 19–28.
[41] Y. Zheng, S. E. Li, J. Wang, L. Y. Wang, and K. Li, "Influence of information flow topology on closed-loop stability of vehicle platoon with rigid formation," in *Proc. 17th Int. IEEE Conf. Intell. Transp. Syst. (ITSC)*, Oct. 2014, pp. 2094–2100.

Carlos Massera Filho (S'14) received the B.Sc. degree in computer engineering from São Carlos School of Engineer in 2012. He is currently working toward the Ph.D. degree with the Institute of Mathematics and Computer Science, University of São Paulo. He has been involved in autonomous and cooperative vehicle control and estimation systems. His research interests are constrained optimal control, robust optimal control, robust convex optimization, and its applications to autonomous and cooperative vehicles.

Marco H. Terra (M'16) received the Ph.D. degree in electrical engineering from University of São Paulo (USP), São Carlos, Brazil, in 1995. He is currently a Full Professor of Electrical Engineering with USP. He has reviewed papers for over 30 journals and to the Mathematical Reviews of the American Mathematical Society. He has authored over 190 conference and journal papers. He has co-authored the book *Robust Control of Robots: Fault Tolerant Approaches* (Springer). His research interests include filtering and control theories, fault detection and isolation problems, and robotics. He was the coordinator of the Robotics Committee and the President of the Brazilian Automation Society. He is an *ad hoc* Referee for the Research Grants Council of Hong Kong.

Denis F. Wolf (M'15) received the Ph.D. degree in computer science from University of Southern California in 2006. He is an Associate Professor with the Department of Computer Systems, University of São Paulo (USP). He is also the Director of the Mobile Robotics Laboratory, USP, and a member of the Center for Robotics, USP. His research interests include mobile robotics, intelligent transportation systems, machine learning, and computer vision.